# A Type-1 Fuzzy Fusion Model based on the Dempster-Shafer Theory for the simulation of 3D Fused Deposition

Wafa' H. AlAlaween<sup>a\*</sup>, Abdallah H. AlAlawin<sup>b</sup>, Belal M.Y. Gharaibeh<sup>a,c</sup>, Mahdi Mahfouf<sup>d</sup>, Ahmad Alsoussi<sup>e</sup>, Saif O. AbuHamour<sup>f</sup> and Ashraf E. AbuKaraky<sup>f</sup>

**Abstract.** In this research, a novel fusion model which incorporates a type-1 fuzzy logic system (T1FLS) and the Dempster-Shafer theory (DST) is proposed to model the 3D fused deposition process. First, the experimental data, which are constructed based on the Taguchi L18 array for two filaments (i.e., Polyether-ether-ketone and Polyether-ketone-ketone), are used to develop T1FLSs that have different structures. Second, a fusion algorithm integrating fuzzy logic and the DST is presented to integrate the predicted values of the T1FLSs after analysing the behaviours of such systems in the space examined. The proposed model can integrate such systems in a way that can resolve possible conflicts among the models developed in the first stage and, as a result, it can improve the predictive performance. Validated on a set of experimental data, the proposed fusion model has improved the predictive performance with an average improvement of 25.6%. The fusion model developed is employed to anticipate the mechanical characteristics of a dental part produced by fused deposition.

Keywords: Dempster-Shafer theory, Fusion model, Taguchi L18 orthogonal array, Type-1 fuzzy logic system

### 1. Introduction

Additive manufacturing, or the so-called 3D printing and rapid manufacturing, is well established as an innovative manufacturing approach for complex manufacturing industries [1-3]. In brief, such an approach involves the generation of complex 3D parts from pre-designed 3D structures by adopting material additive processes including, for instance, layer-by-layer or surface-by-surface ones [4]. In addition to its considerable effect on innovation and the manufacturing and its related industries, additive manufacturing is considered to be a vital constituent of the In-

dustry 4.0 revolution because of its (i) characteristics that facilitate low-volume but cost-effective manufacturing; (ii) ability to generate highly complex monolithic structures; and (iii) capability of handling changes and, thus, allowing flexible production of customized 3D printed parts using different colours and materials at small as well as large scales [5-8]. Consequently, many research studies have been directed to investigate the various 3D printing techniques across a vast myriad of industries including, but not limited to, aerospace, pharmaceutics and tissue engineering [9-12]. Various state-of-the-art techniques have been, in general, covered under the um-

<sup>&</sup>lt;sup>a</sup> Department of Industrial Engineering, The University of Jordan, Amman, Jordan.

<sup>&</sup>lt;sup>b</sup> Department of Industrial Engineering, Faculty of Engineering, The Hashemite University, Zarqa, Jordan.

<sup>&</sup>lt;sup>c</sup> Collage of Engineering and Applied Sciences, American University of Kuwait, Salmiya, Kuwait.

<sup>&</sup>lt;sup>d</sup> Department of Automatic Control and Systems Engineering, The University of Sheffield, Sheffield, UK.

<sup>&</sup>lt;sup>e</sup> Printie 3D, Amman, Jordan.

<sup>&</sup>lt;sup>f</sup> Department of Oral and Maxillofacial Surgery, Oral Medicine and Periodontology, The University of Jordan, Amman, Jordan.

<sup>\*</sup>Corresponding author. E-mail: w.alaween@ju.edu.jo

brella of additive manufacturing. Such techniques include fused deposition modelling (FDM), resin printing (i.e., stereolithography (SLA)) and selective laser sintering (SLS) [13-16]. FDM, whose essence is the production of 3D printed parts by controllably depositing liquefied thermoplastic polymer layers, is considered to be one of the most common techniques in various applications (e.g., biomedical science) [17]. This is because of the ability of the FDM process to deal with different biomedical polymers (e.g., Polyether-ether-ketone (PEEK) and Polyether-ketone-ketone (PEKK)) [18]. Thus, many studies have concentrated on the FDM process and its various applications.

The various parts and polymers 3D printed using FDM for various applications, in particular, biomedical ones were examined in order to replace the aggravated autograft and allograft ones [17]. Polylactic acid (PLA) scaffolds, for example, were 3D printed by employing the FDM technique under different sets of FDM parameters, in order to examine their properties [18]. Furthermore and to enhance its quality attributes and imitate the human bone structure, PLA was amalgamated with polyvinyl alcohol, thermalstimulus-based hydroxyapatite and nanohydroxyapatite and, then, used to produce scaffolds. The properties of such scaffolds (e.g., mechanical and rheological properties) were analysed and then compared to the PLA ones [9, 19-22]. In addition, various orthopaedic and dental 3D printed parts were produced using the FDM process by PEEK and carbon-fibrereinforced PEEK, and their mechanical and biocompatibility characteristics were assessed [23]. Since various parameters can play a significant role in defining the fate of the final 3D printed parts, several research papers investigated these parameters. These parameters can be, in general, categorised into: (i) material-related parameters such as the mechanical and rheological characteristics of the polymers; (ii) process-related parameters such as humidity; and (iii) machine-related parameters such as print speed [11, 24]. To design and print 3D printed parts having the required quality attributes, such parameters need to be controlled and optimized. Therefore, a spectrum of experimental techniques has been proposed to control and optimize these parameters [25]. An analytical paradigm was, for instance, developed to assess the combinatory influences of the material- and machine-related parameters on the attributes of 3D printed specimens [26]. Likewise, the effects of various parameters such as orientation, print speed and infill type on the attributes of 3D printed PLA parts were statistically analysed by determining the correlation coefficient and the P-value using the analysis of variance test [27-31]. Moreover, the impact of copper electroless plating on 3D printed specimens produced using the acrylonitrile butadiene styrene (ABS) polymer was also studied [32]. Furthermore, digital imaging was utilized to show how the mechanical attributes of the 3D printed parts were affected by different thickness values [33]. Likewise, the influences of four FDM parameters, namely, layer thickness, raster angle, infill density, and nozzle temperature on the mechanical properties were examined for PLA, ABS and Chlorinated Polyethylene (CPE) polymers [34]. In addition, the influence of the infill pattern on fatigue life of 3D printed parts produced using ABS was studied by examining various infill pattern geometries [35]. It was proved by comparative evaluation of the determined fatigue life that infill pattern geometries had considerable effects on fatigue life [35].

Nowadays, there is a strong need to anticipate the quality characteristics of 3D printed specimens accurately, in particular, in biomedical science, pharmaceutics and tissue engineering. Therefore, several studies have been devoted to implementing and developing systems-engineering paradigms that can simulate the FDM process. For instance, various multi-criteria decision-making paradigms (e.g., VIKOR) were employed to determine the best combination of the FDM parameters [36, 37]. In addition, the genetic algorithm was embedded in the structure of the artificial neural network to anticipate the strength of 3D printed specimens prepared using various polymers [38-41]. Furthermore, a modelling structure based on conceptual modelling and neural networks was proposed to better understand and, consequently, model the FDM process. For instance, an artificial neural network was designed to represent the mechanical attributes of three polymers (i.e., PLA, ABS and CPE) as a function of four FDM parameters [34]. In addition, an interval type-2 fuzzy logic system (IT2FLS) was designed to mimic the FDM process and to handle the uncertainties in the measurements of the quality attributes of the 3D printed parts [42]. Such a system had the ability to predict the quality attributes of the 3D printed parts and provide a linguistic understanding of the relationships between the FDM parameters and the quality attributes. However, the performance of such a system was represented by the average predicted performance for all the areas in the space examined. In other words, the system behaviours at different areas in the spaces examined cannot be shown. In addition, a modelling paradigm based on basis functions was designed to mimic the FDM process and predict the attributes of the parts produced [43]. Such a paradigm consisted of a number of radial basis functions that play an integral role in extracting the relationships between the FDM parameters and the attributes examined. However, such a paradigm cannot handle uncertainties and cannot provide users with linguistic representation of the relationships extracted. Furthermore, some research papers have focused on optimizing the FDM process and its different parameters [44, 45]. For instance, the process was optimized by defining the different challenges faced while printing polymers, composites, geopolymers and novel materials, where machine parameters were investigated to optimize printing novel polymers for various applications [44]. Likewise, a right-first-time concept-based paradigm that integrated fuzzy logic and multiobjective swarm optimization was proposed to define the best FDM parameters that need to be employed to 3D print parts with predefined mechanical attributes with minimum waste and recycling ratios [45].

Although a huge body of research has concentrated on understanding and modelling the FDM process, and mapping the quality attributes of the 3D printed parts to the FDM parameters, there is an urge to develop a paradigm that can (i) accurately predict the quality attributes for a highly dimensional space resulted from the considerable number of the FDM parameters that affect these attributes; (ii) deal with a limited number of sparse data points because of the cost and time required to produce more 3D printed test specimens; and (iii) handle measurement uncertainties. Ascertaining all these features may not be possible with a single paradigm. Therefore, in this paper, a novel fusion model that incorporates the Dempster-Shafer theory (DST) and a type-1 fuzzy logic system (T1FLS) is presented to simulate the FDM process and study the effects of the process parameters on the mechanical characteristics of the parts produced using PEEK and PEKK. The fusion model is developed to (i) integrate various T1FLSs that have different structures developed to represent the FDM process, such systems can play an integral role in extracting all possible relationships between the process parameters and the mechanical characteristics; (ii) examine the behaviours of these systems in the space investigated instead of representing the predictive performance by its average values in the different areas of the space; (iii) resolve possible conflicts among the various T1FLSs; (iv) improve the modelling predictive performance in the areas with

unacceptable performance by considering the systems that provide the best predictive performance; and (v) tackle measurement uncertainties by employing T1FLS and the DST. The paper is structured as follows. Section 2 briefly summarizes the equipment used and the experimental work. The development of the proposed fusion model and the mathematics behind the DST and the T1FLS are discussed in Section 3, whereas its results are summarized in Section 4. Conclusions are, then, listed in Section 5.

### 2. Experimental Work

Two types of polymers (i.e., engineering-grade PEEK and PEKK) filaments were studied in this paper. PEEK and PEKK are both semicrystalline thermoplastic high-temperature polymers that have relatively excellent mechanical as well as chemical resistance characteristics. Such polymers were provided by 3DXTECH (Michigan, USA). ASTM-D638 parts were produced using the FUNMAT HT 3D printer, as a functional-materials FDM printer, as shown in Figure 1, (INTAMSYS Technology Inc., Minneapolis, USA). Such a printer is supported by InstamSuite 3.6.2 program that was employed to convert the 3D designed structure of the ASTM-D638 parts to a GCODE format. The ASTM-D638 parts were printed using various sets of operating conditions. In addition to the three mechanical characteristics studied in this paper, the eight FDM parameters with the identified levels, which were studied for PEEK and PEKK, are listed in Table 1.



Figure 1 The FUNMAT HT 3D printer.

Table 1 The fused deposition modelling parameters and the mechanical characteristics [40].

Parameters	eters Levels Mechanical characteristics		Devices' parameters	
Infill pattern	Cubic and grid	Tensile strength (MPa)	Load: 50KN and speed:	
Thickness	0.1, 0.15 and 0.2 μm	Elongation (%)	1mm/min	
Density	20, 60 and 100%	, ,		
Speed	10, 30 and 50mm/s	Micro-hardness	Load: 0.98N and time: 15	
Number of shells	1, 2 and 3		seconds	
Cooling rate	0%, 50% and 100%			
Orientation	0°, 45° and 90°			
Raster width	0.25, 0.4 and 0.6um			

The Taguchi L18 array was utilized to understand the relationships and to model the FDM process.

Therefore, 18 experiments were carried-out for each polymer. To ensure good repeatability, each experiment was repeated three times. Once they were printed, the specimens were removed from the printer glass plate. According to manufacturer recommendations, all specimens produced were annealed. The mechanical attributes were experimentally estimated. The micro-hardness was measured using the micro Vickers hardness (HTMV 2000M, echo LAB, Italy) with load and time values of 0.98 N and 15 seconds, respectively. Whereas the ultimate tensile strength and elongation were determined using Instron (SHI-MADZU, USA) with load and speed values of 50 kN and 1 mm/min, respectively. The parameters of these apparatuses are summarized in Table 1. For each experiment, the average of the three repetitions was then estimated.

For the various sets of the FDM parameters, various fracture patterns occurred at different locations. It was apparent that the investigated parameters have various influences on the mechanical attributes examined in terms of the nature of the relationships and their strength, which were proved by calculating the correlation values that are listed in Table 2. Such coefficients are reasonable. In addition, some of the FDM parameters have different correlation values for

PEEK and PEKK. To elucidate, the layer thickness has a negligible impact on the strength for PEEK, however it has a significant one on that for PEKK. It also has a considerable effect on the elongation for PEKK but a negligible one for PEEK. It is also worth noting that the relationships between the layer thickness and the strength for PEEK and PEKK are direct and indirect, respectively. Likewise, the relationships between the layer thickness and the elongation for PEEK and PEKK are direct and indirect, respectively. Moreover, different natures of the relationships can be seen between the FDM parameters and the mechanical attributes examined. For instance, the relationships between the print speed and specimens' strength for PEEK and PEKK are indirect and direct, respectively. In addition, the layer thickness had direct and indirect effects on micro-hardness for PEEK and PEKK, respectively. It is also apparent that the layer orientation can considerably affect the strength and elongation. However, it has an inconsiderable impact on micro-hardness for both materials. For the infill pattern, the analysis of variance was used to study its influences. It was found that it significantly affected the mechanical attributes examined with Pvalues of less than 0.05. It was found that the Pvalues for the ultimate tensile strength, elongation and microhardness are 0.032, 0.030 and 0.027.

Table 2 The correlation coefficients.

Parameters	PEEK			PEKK		
	Strength	Elonga- tion	Micro- hardness	Strength	Elonga- tion	Micro- hardness
Thickness	0.04	0.30	0.14	-0.16	-0.09	-0.18
Density	0.68	-0.42	-0.22	0.39	-0.26	0.02
Speed	-0.20	-0.21	0.03	0.22	-0.38	-0.61
Number of shells	0.22	0.00	-0.41	0.50	0.20	-0.16
Cooling rate	0.04	0.20	-0.51	-0.21	0.07	-0.10
Orientation	0.10	0.22	0.05	-0.08	-0.44	-0.05
Raster width	0.33	0.56	-0.15	0.43	-0.25	-0.27

# 3. A Fuzzy Fusion Model

The advances in the computing power that have been witnessed recently make data-driven models an ideal way to represent and model complex processes, in particular, when physical models are difficult to derive and/or implement [46]. This has been the main reason behind the extensive use of various datadriven models such as linear regression, artificial neural networks and fuzzy logic in various areas including, for example, pharmaceutics, medicine, automobile, supply chain and manufacturing [47-49]. The core of these models, as the name indicates, rests with data in terms of the amount of data available as well as the distribution in the space investigated [50, 51]. To elucidate, having a good number of data points is of paramount importance to extract and simulate the inputs/outputs relationships of a process. In addition, a good distribution of the data in the space examined can prevent developing a biased paradigm that can perform satisfactorily in those areas where the amount of data is enough and unsatisfactorily elsewhere [52]. Therefore, integrating several models that may have different structures can circumvent these challenges and help in extracting relationships that may not be extractable using a single model. However, integrating different models is not as simple as it may sound, as one needs to consider the behaviours of the models in the space examined and, thus, integrate them in a way that can improve the predictive performance [53]. Various paradigms can be employed to integrate different models. Information fusion, as a concept that simulates the human cognitive process, is considered to be one of the effective ways of integrating information from different sources in a way that improves the reliability of such information and, thus, allows decision makers to take optimal decisions [54].

Among the various algorithms presented in the related literature, the DST is considered to be an efficient one, this being due to its ability to consider imprecision and possible conflicts among various sources of information [53]. However, the DST deals only with uncertainties due to probabilities and due to lack of specifications. Therefore, and in order to tackle the uncertainties due to fuzziness, an information fusion algorithm based on both fuzzy logic and the DST is presented in this research, and incorporated with the T1FLS to (i) integrate various

T1FLSs that have different structures; (ii) examine the different behaviours of the T1FLSs developed to simulate the FDM process in the space investigated; (iii) resolve possible conflicts among the various T1FLSs; and (iv) improve the modelling predictive performance, in particular when the data available are limited and/or sparse.

Figure 2 depicts the schematic structure of the proposed fuzzy fusion model that incorporates the DST and the T1FLS. The proposed structure consists of several stages. First, the experimental data are used to develop M T1FLSs that include different architectures (i.e., the number of fuzzy sets and fuzzy parameters). Such T1FLSs can capture the process behaviours represented by the data and act synergetically when simulating and extracting the possible behaviours of the process in the space examined. Second, based on the predicted outputs obtained from the T1FLSs developed, the fusion algorithm is implemented to integrate the predicted outputs of the T1FLSs. The behaviours of the T1FLSs that have different structures are evaluated in the space investigated by clustering the performance of these models into several clusters described linguistically (e.g., Unsatisfactory, Satisfactory and Excellent). For each predicted output, the membership degrees are then estimated with respect to these clusters. Then, the mass functions are assigned. Such a step is followed by combining the hypothesis which are the clusters indicating the performance of the T1FLSs. In this structure, a hypothesis of one T1FLS should be combined with another hypothesis that has an equal or better predictive performance value. In other words, a high level of conflict needs to be assumed between a hypothesis and a one with low predictive performance. This can improve the predictive performance. The membership degrees with respect to the combined hypotheses are then calculated and defuzzified to determine the final predicted outputs.

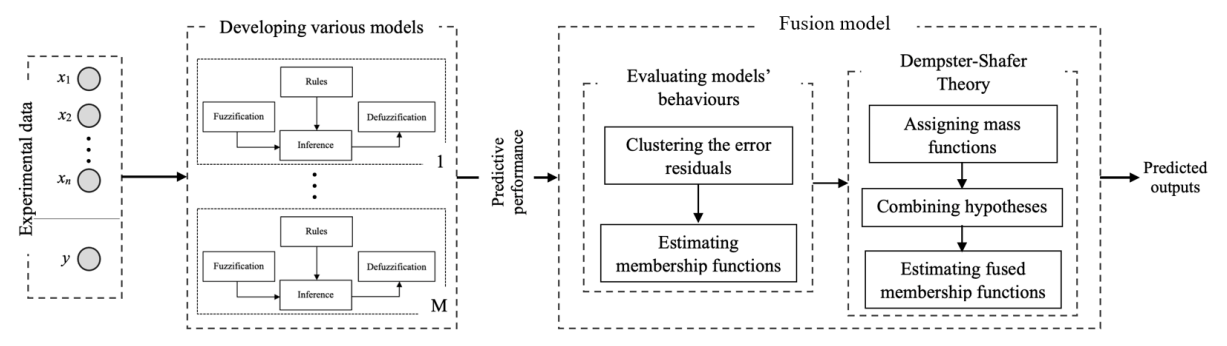


Figure 2 The schematic structure of the fuzzy fusion model.

The mathematics behind the proposed fuzzy fusion model can be presented by including the mathematics behind the T1FLS and the DST based on fuzzy logic. Although the mathematics behind them have been publicised [53-56], in this research, the key developments are briefly summarized.

### 3.1. Type-1 Fuzzy Logic System

Nowadays, fuzzy systems have been used to simulate and represent complicated processes using data provided and/or expert knowledge, this being due to their ability to (i) represent the relationships among inputs and outputs; (ii) handle process uncertainties by using fuzzy sets; and (iii) expand the linguistic representation of a process by extracting fuzzy If/Then rules that can be employed to control such a process. Therefore, they have been utilized in many applications such as supply chain and pharmaceutics [47]. Among the various fuzzy systems in the related literature, the T1FLS is utilized in this research paper because of its simplicity.

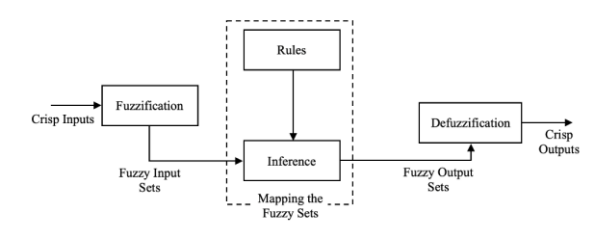


Figure 3 The T1FLS structure.

Figure 3 depicts the representation of the T1FLS, which contains four steps: fuzzification, inference, extracting rules and defuzzification. First, the process inputs, which are commonly in the crisp/singleton form  $(x_1, x_2 ... x_n)$ , are fuzzified to identify the fuzzy

inputs (i.e.,  $A_i^i$  that stands for the  $i^{th}$  fuzzy set of the

*j*<sup>th</sup> parameter). They are expressed in the form of membership functions. Various membership functions (e.g., triangular and trapezoidal) have hitherto been utilized. Due to its continuity, the Gaussian membership function is exploited in this work. It can be represented as follows:

$$\mu_j^i(x_j) = \exp\left[-\frac{1}{2}\left(\frac{x_j - m^i}{\sigma^i}\right)^2\right] \tag{1}$$

where  $m^i$  and  $\sigma^i$  stand for the mean and the standard deviation of the  $i^{th}$  fuzzy set, respectively. Once the crisp inputs are fuzzified, the output sets ( $B^i$ ) are written as functions of the fuzzy input sets via the inference process which utilizes the extracted or provided IF/Then rules. Such rules are linguistically presented as follows:

**Rule<sup>i</sup>:** IF 
$$x_1$$
 is  $A_1^i$  ... and  $x_n$  is  $A_n^i$ , THEN  $y$  is  $B^i$ .

Application-wise, a single output is needed, therefore, the output fuzzy set is defuzzified via the many techniques already available. In this research article, the centroid defuzzifier was utilized.

# 3.2. Dempster-Shafer Theory

Information fusion is considered to be one of the main cognitive processes employed by human to integrate information from different sources. Such a process aims to realise efficient inferences that lead to making the best decision [56]. The need for such a process stems from the fact that (i) information obtained from a single source may be limited; and (ii) information accuracy may not be as required [57]. It has been utilized in different areas such as medical,

marine and manufacturing to enhance the reliability and accuracy of information provided [57].

Various information fusion algorithms have been proposed in the literature. Such algorithms include Bayesian, fuzzy logic and the DST [57]. Among the various algorithms presented, the DST is considered to be an efficient one, this being due to its ability to take into consideration imprecision and resolve possible conflicts among various sources of information [53]. However, the DST can only consider uncertainties due to probabilities and lack of specification [53]. However, in order to develop a reliable and effective fusion paradigm, three types of uncertainties due to probabilities, lack of specification and fuzziness need to be carefully considered [53]. However, the DST can only deal with the first two types of uncertainties. Therefore, in this research article, a paradigm that integrates the DST and fuzzy logic is presented, where the third type of uncertainties can be dealt with using fuzzy logic.

# 3.3. Dempster-Shafer Theory Based on Fuzzy Logic

In general, the DST, or the so-called the evidence theory, is a commonly used framework in the cognitive process for reasoning with uncertainties. Such a theory can only handle uncertainties due to probabilities and lack of specifications. In addition, determining the mass function of the hypothesis to be combined is considered to be a challenge in performing the DST [53, 56]. It can be estimated using various approaches including distance or probabilities. In order to circumvent such a challenge and consider uncertainties due to fuzziness, the DST is integrated with fuzzy logic in this research to successfully identify the mass function.

The hypotheses are identified based on the performance of the predictive models in the space investigated. The performance of the developed models is measured using the error residuals. In this research paper, unsupervised clustering is utilized to identify such hypotheses by classifying the predictive performance values into three classes: Unsatisfactory, Satisfactory and Excellent. The input parameters and the error values for each data point from all the models developed are then classified. The membership degree for each point is calculated with respect to the three clusters as follows:

$$\mu_i^e = \exp\left(-\frac{1}{2}\left(\frac{x_i^e - m^e}{\sigma^e}\right)^2\right) \tag{2}$$

where  $x_i^e$  represents the residual error of the  $i^{th}$  data

point and the rest of the parameters used are as identified in Section 3.1. The superscript (e) is employed to distinguish the error residuals related parameters of the DST from those used to develop the T1FLSs presented in Section 3.1 Such membership degrees are then utilized to estimate the mass function as follows [56]:

$$m_{p} = \left(1 - \sum_{\substack{j=1\\j \neq t}}^{J_{\text{max}}} \mu_{j}^{e} \times (\eta - \mu_{j}^{e})\right) \times \mu_{p}^{e}$$
(3)

$$\xi = \arg \max_{1 \le j \le J_{\text{max}}} \mu_j^{j}$$

 $\xi = \arg\max_{1 \leq j \leq J_{\max}} \mu_j^e$  where  $m_p$  and  $\xi$  stand for the mass function of the

pth hypothesis (i.e., clusters) and the maximum membership function, respectively. Various hypotheses (i.e., H<sub>1</sub>, H<sub>2</sub> ... H<sub>Jmax</sub>) can then be integrated using Eq(4).

$$m_{F} = \frac{1}{1 - K} \times \sum_{H_{1} \cap H_{2} \cdots H_{J_{\max}} \neq \emptyset} \left( \prod_{1 \leq j \leq J_{\max}} m_{j} \right)$$

$$K = \sum_{H_{1} \cap H_{2} \cdots H_{J_{\max}} = \emptyset} \left( \prod_{1 \leq j \leq J_{\max}} m_{j} \right)$$

$$(4)$$

where  $m_E$  represents the mass function of the fu-

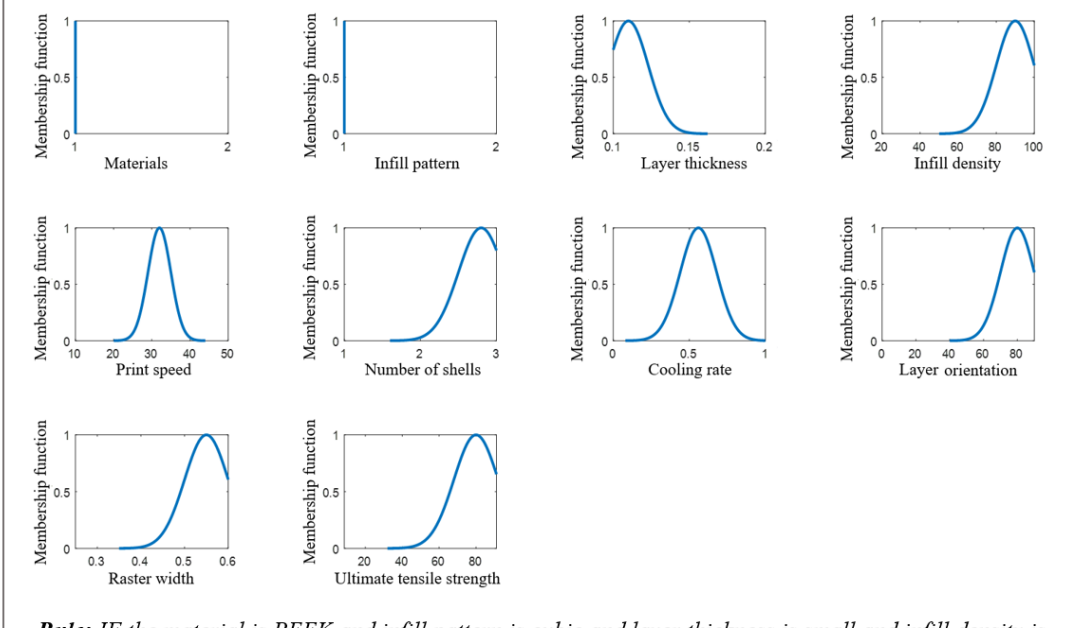
sion model. A measure of conflict is denoted K, which is also utilized to determine the normalization factor (i.e., 1-K). It is worth emphasising that a hypothesis of a model needs to be integrated with the hypotheses of other models that have the same or better predictive performance. This can lead to improving the predictive performance. To illustrate, a Satisfactory cluster of a T1FLS can only be combined with Satisfactory and Excellent clusters of the other T1FLSs, a considerable conflict value is assumed between such a cluster and the Unsatisfactory ones of the other T1FLSs. Once the mass functions are calculated for the three clusters, the membership functions are then estimated and used to estimate a defuzzified predicted output using the height defuzzifier presented in [58].

### 4. Implementation and Results

# 4.1. Fusion Model: Implementation and Results

In this research work and as depicted in Figure 2, 10 T1FLSs that have different structures, as previously stated, were developed for each output (i.e., a mechanical characteristic). Each T1FLS was established by partitioning the data into training (28) and testing (8) sets. The training and testing sets are generally utilized to extract the relationships and evaluate the T1FLS's generalization capabilities, respectively [47]. The training and testing sets of the 10 T1FLSs have the same numbers of data points. However, such points have different distributions in the space examined. Therefore, the various T1FLSs developed can simulate the input/output relationships. To develop a representative system for the FDM process, the FDM parameters needs to be carefully considered. For instance, material type and infill pattern were considered as singleton variables (i.e., crisp or discrete), whereas the remaining FDM parameters were considered as continuous variables. Various numbers of rules were examined for each T1FLS. The optimal one that was chosen was the one that provided the optimal predictive performance determined by the root mean square error (RMSE) (i.e., the minimum RMSE value). For a specific number of rules, the system's parameters were initially assigned via the hierarchical approach presented in [59]. These parameters were then optimized during the training process by utilizing the steepest descent procedure that was embedded in the back-propagation paradigm [58].

For the ultimate tensile strength, 11 rules, as the best number of rules, were used to develop the T1FLS. Figure 4 shows an example of one of these rules. The linguistic representation of such a rule is presented in Figure 4.



Rule: IF the material is PEEK and infill pattern is cubic and layer thickness is small and infill density is high and print speed is medium and number of shells is high and cooling rate is medium and layer orientation is high and raster width is high, THEN the ultimate tensile strength is high.

Figure 4 One of the 11 rules used for the ultimate tensile strength rule (Materials (1) PEEK and (2) PEKK; Infill pattern (1) Cubic and (2) Grid).

Figure 5 shows the predictive performance for one of the T1FLSs developed using 11 rules, as the best number of rules for this system. The RMSE values for training and testing sets are 9.65 MPa and 8.97 MPa, respectively, whereas the R<sup>2</sup> values for the corresponding sets are 0.81 and 0.78, respectively. Such performance measures represent the average values of all points, in other words, they do not show how the model behaves in the space examined. To elucidate, it is apparent from Figure 5 that 14 data points in the training set out of 28 and 4 data points in the testing set out of 8 lay outside the 90% confidence interval. Furthermore, the data points in both sets are scattered around the best-fit line. Such behaviours were not detected by looking at both the RMSE and R<sup>2</sup> values. Such behaviours can be attributed to (i) the highly nonlinear relationships between the FDM parameters and the ultimate tensile strength; (ii) the limited number of data points that are used to develop a T1FLS, as a data-driven model; and (iii) the number of input parameters (i.e., nine) examined which can result in the phenomenon of the "curse of dimensionality" when the data points are limited. Therefore, and based on the results of the 10 T1FLSs developed that have similar behaviours to the system presented in Figure 5 but different in the space examined, it was obvious that a single T1FLS cannot be used to simulate the FDM process and anticipate the mechanical characteristics using such limited data points. Therefore, there is a need for the new fusion model presented in Section 3.

Once the 10 T1FLSs were developed, their performance behaviours in the space were classified into the three abovementioned classes using the k-means clustering algorithm. Therefore, the FDM parameters and the residuals of these 10 T1FLSs were employed to identify the behaviours of the models (i.e., areas where the performance of a model is Unsatisfactory, Satisfactory and Excellent). The parameters of the identified clusters were estimated. Figure 6 depicts the membership functions for these three clusters with their parameters for the 10 T1FLSs developed.

Figure 7 shows how one of the developed T1FLSs behaved in an area for the strength. It indicates that the performance of such a T1FLS is Excellent when the material is PEEK, infill pattern is grid, layer thickness is high, infill density is high, print speed is high, number of shells is medium, cooling rate is small, layer orientation is 45° and raster width is medium.

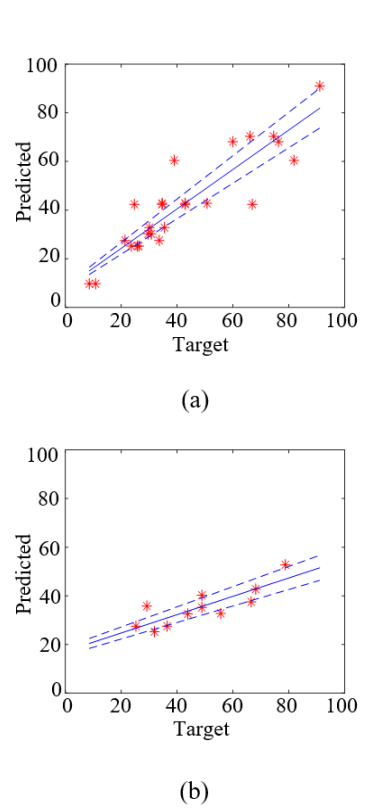


Figure 5 The performance of a T1FLS for the ultimate tensile strength with a 90% confidence level: (a) Training and (b) Testing sets.

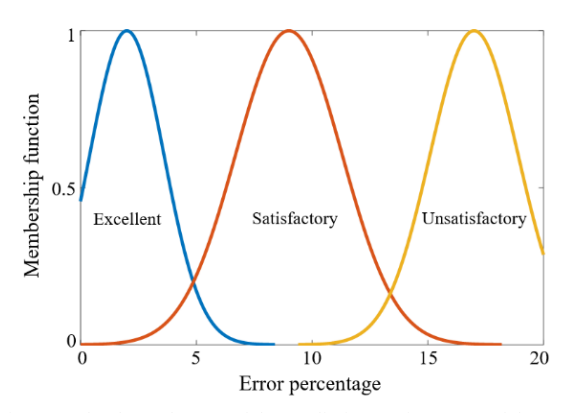


Figure 6 The three clusters of the predictive performance of the T1FLSs.

Based on the identified clusters for the 10 T1FLSs, the defined membership was utilized to determine the mass functions, as described in Section 3. Such mass functions were then integrated as mathematically shown in Equation (4) in order to find the ones for the fusion model that integrated the 10 T1FLSs. Then, the membership function values of such a model were estimated by numerically solving Equation (3).

Finally, the outputs were then determined by the height defuzzification. Figure 8 depicts the performance of the proposed fusion model for the strength, where the RMSE (training, testing) and R<sup>2</sup> (training, testing) are [3.57, 6.99] MPa and [0.96, 0.96], respectively. The testing RMSE value is twice the training one. However, such a high value is due to that 6 data points that have values of 60MPa or greater, whereas the majority of the data points in the training set have values that are less than 60MPa. Therefore, such a high value is not due to overfitting. This can be proven by looking at the R<sup>2</sup> values. It is apparent that the performance of such a newly model outperformed the single system with an average overall improvement of 20% in R<sup>2</sup> for the ultimate tensile strength. It is also noticeable that all the points are within the confidence band. Furthermore, they are scattered neatly around the best-fit line.

In a similar manner, a T1FLS and the fusion model based on 10 T1FLSs were utilized to predict the elongation values and micro-hardness. The predictive performance for these models is listed in Table 3. Such a table shows that the predictive performance values of T1FLSs developed for both elongation and micro-hardness were not acceptable. Therefore, the fusion model was used to improve the predictive per-

formance. The performance values of the fusion models developed for the two mechanical characteristics are better than those of the T1FLSs with average overall improvements of 27% and 30% in R<sup>2</sup>, respectively.

For comparison purposes, IT2FLS and the radial based integrated network presented in [42] and [43], respectively, were employed to predict the three mechanical characteristics. The results obtained are also summarized in Table 3. It is noticeable that the fusion model outperformed these models with a considerable improvement. This can be attributed to (i) its structure that consists of several T1FLSs that can play an integral role in extracting and representing the relationships between the FDM parameters and the mechanical characteristics; (ii) its ability to analyse the behaviours of these systems in the different areas of the space examined; and (iii) its ability to integrate the predicted outputs in these areas in a way that can improve the predictive performance. In addition, the fusion model can provide a linguistic understanding of the relationships between the FDM parameters and the mechanical characteristics that can be utilized to control and understand the process.

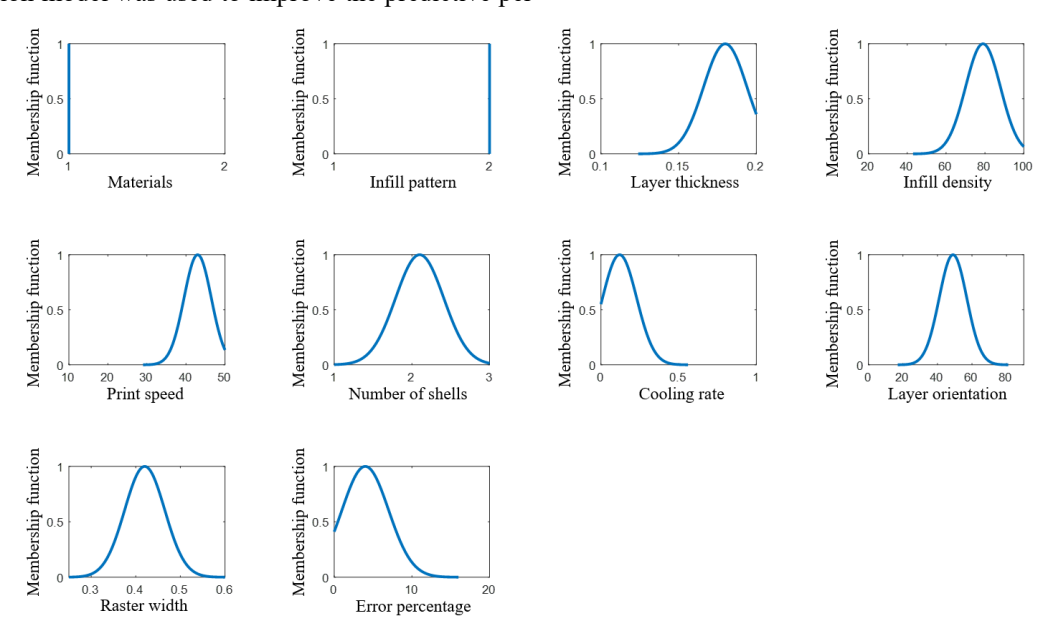


Figure 7 The performance of a T1FLS in the space area of the ultimate tensile strength.

Table 3 The performance values.

Model			Strength (MPa)	Elongation (%)	Microhardness
TIFLS —	$\mathbb{R}^2$	Train	0.81	0.74	0.71
	K	Test	0.78	0.75	0.7
	RMSE	Train	9.65	5.8	2.76
	RMSE	Test	8.97	5.8	2.85
ITOEL C	$\mathbb{R}^2$	Train	0.88	0.8	0.76
	K-	Test	0.87	0.81	0.75
IT2FLS	RMSE	Train	6.57	4.48	2.27
	KWSE	Test	6.79	4.51	2.28
Integrated network	$\mathbb{R}^2$	Train	0.94	0.93	0.90
		Test	0.91	0.91	0.91
	RMSE	Train	5.4	2.3	1.30
		Test	5.9	7.6	1.40
Fusion model	$\mathbb{R}^2$	Train	0.96	0.94	0.92
	K <sup>2</sup>	Test	0.96	0.95	0.93
	RMSE	Train	3.57	3.72	1.41
		Test	6.99	3.71	1.38

# 4.2. Model Verification: Medical Applications

The capabilities of the fusion paradigm in anticipating the three mechanical characteristics of the 3Dprinted parts were demonstrated by predicting these attributes for a dental implant (i.e., MidFace Rim) presented in Figure 9. Such a part was produced by the same printer mentioned in the second section using PEEK. The printing parameters in terms of infill pattern and its density, thickness, printing speed, number of shells, cooling rate, printing orientation and raster width were cubic, 100%, 0.12mm, 20mm/s, 3, 0%, 0° and 0.4mm, respectively. It is worth noting that measuring the strength and elongation for such a part, which is not printed according to the specifications of the standard test parts, is not as simple as it may seem and may not provide accurate measurements. Therefore, the new fusion model can be employed in this case and perhaps similar ones to anticipate these attributes. Therefore, the mechanical characteristics were predicted using the fusion models developed in Section 4.1. The anticipated values of the MidFace rim were 102.4MPa, 19.5 and 29.3 for the strength, elongation and micro-hardness respectively. The average of measured values of the micro-hardness for the MidFace Rim is 30.5 which is close to the anticipated one (i.e., 29.3).

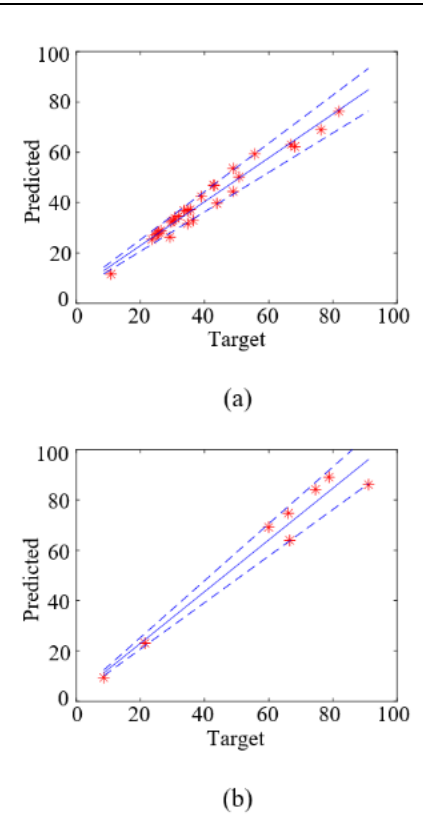


Figure 8 The predictive performance of the proposed fused model for the strength with a 90% confidence band: (a) Training and (b)

Testing sets.



Figure 9 MidFace Rim.

### 5. Conclusion

A novel fusion model based on incorporating a type-1 fuzzy logic system (T1FLS) and the Dempster-Shafer theory (DST) was presented in this research article to simulate the 3D fused deposition process. Such a model was developed in two stages. First, several T1FLSs having different structures were developed. Second, the fuzzy based DST was employed to integrate the predicted outputs of the T1FLSs after analysing their behaviours in the space examined. In addition to integrating and analysing the behaviours of the T1FLSs, such a model can resolve possible conflicts among these systems and, as a result, can lead to a better predictive performance. In summary, the fusion model presents a promising advancement not only in 3D printing and its techniques but also in other equally complex processes with highly dimensional spaces and a limited number of sparsely distributed data points. In the future, the fusion model can be incorporated with multi-objective optimization paradigms in order to identify the best 3D printing parameters that need to be employed to produce 3D printed specimens with predefined attributes. This incorporation can lead to minimizing waste and recycling ratio and reducing time-to-market.

# **Conflicts of Interest**

The author(s) declare(s) that there is no conflict of interest regarding the publication of this paper.

# **Funding Statement**

This work was supported by The Royal Academy of Engineering (UK) and Industrial Scientific Research and Development Fund-The Higher Council for Science and Technology (Jordan) for the financial support (Grant TSP1134).

This work was also supported by Abdul Hameed Shoman Foundation (Grant 230800045).

### Acknowledgment

The authors would like to thank The Royal Academy of Engineering (UK) and Industrial Scientific Research and Development Fund-The Higher Council for Science and Technology (Jordan) for the financial support.

The authors would like to thank Abdul Hameed Shoman Foundation for the financial support.

### References

- [1] G. N. Levy, R. Schindel, and J.-P. Kruth, "Rapid manufacturing and rapid tooling with layer manufacturing (LM) technologies, state of the art and future perspectives," *CIRP annals*, vol. 52, no. 2, pp. 589-609, 2003.
- [2] S. H. Huang, P. Liu, A. Mokasdar, and L. Hou, "Additive manufacturing and its societal impact: a literature review," *The International Journal of Advanced Manufacturing Technology*, vol. 67, no. 5, pp. 1191-1203, 2013.
- [3] B. P. Conner *et al.*, "Making sense of 3-D printing: Creating a map of additive manufacturing products and services," *Additive Manufacturing*, vol. 1, pp. 64-76, 2014.
- [4] P. Patil, D. Singh, S. J. Raykar, and J. Bhamu, "Multi-objective optimization of process parameters of Fused Deposition Modeling (FDM) for printing Polylactic Acid (PLA) polymer components," *Materials Today: Proceedings*, vol. 45, pp. 4880-4885, 2021.
- [5] M. Doshi, A. Mahale, S. K. Singh, and S. Deshmukh, "Printing parameters and materials affecting mechanical properties of FDM-3D printed Parts: Perspective and prospects," *Materials Today: Proceedings*, 2021.
- [6] A. Cano-Vicent et al., "Fused deposition modelling: Current status, methodology, applications and future prospects," Additive Manufacturing, vol. 47, p. 102378, 2021.
- [7] L. Murr, "Metallurgy of additive manufacturing: Examples from electron beam melting," *Additive Manufacturing*, vol. 5, pp. 40-53, 2015.
- [8] O. Ivanova, A. Elliott, T. Campbell, and C. Williams, "Unclonable security features for additive

- manufacturing," *Additive Manufacturing*, vol. 1, pp. 24-31, 2014.
- [9] M. Alizadeh-Osgouei, Y. Li, A. Vahid, A. Ataee, and C. Wen, "High strength porous PLA gyroid scaffolds manufactured via fused deposition modeling for tissueengineering applications," *Smart Materials in Medicine*, vol. 2, pp. 15-25, 2021.
- [10] E. Boesch, A. Siadat, M. Rivette, and A. A. Baqai, "Impact of fused deposition modeling (FDM) process parameters on strength of built parts using Taguchi's design of experiments," *The international journal of Advanced Manufacturing technology*, vol. 101, no. 5, pp. 1215-1226, 2019.
- [11] C. Parulski, O. Jennotte, A. Lechanteur, and B. Evrard, "Challenges of fused deposition modeling 3D printing in pharmaceutical applications: Where are we now?," Advanced Drug Delivery Reviews, vol. 175, p. 113810, 2021.
- [12] D. B. Short, "Use of 3D printing by museums: educational exhibits, artifact education, and artifact restoration," 3D Printing and Additive Manufacturing, vol. 2, no. 4, pp. 209-215, 2015.
- [13] C. W. Hull, "Apparatus for production of threedimensional objects by stereolithography," ed: Google Patents, 1986.
- [14] C. R. Deckard, "Method and apparatus for producing parts by selective sintering," ed: Google Patents, 1989.
- [15] S. S. Crump, "Apparatus and method for creating threedimensional objects," ed: Google Patents, 1992.
- [16] E. M. Sachs, J. S. Haggerty, M. J. Cima, and P. A. Williams, "Three-dimensional printing techniques," ed: Google Patents, 1993.
- [17] S. Singh, C. Prakash, and S. Ramakrishna, "3D printing of polyether-ether-ketone for biomedical applications," *European Polymer Journal*, vol. 114, pp. 234-248, 2019.
- [18] D. Singh, A. Babbar, V. Jain, D. Gupta, S. Saxena, and V. Dwibedi, "Synthesis, characterization, and bioactivity investigation of biomimetic biodegradable PLA scaffold fabricated by fused filament fabrication process," *Journal of the Brazilian Society of Mechanical Sciences and Engineering*, vol. 41, no. 3, pp. 1-13, 2019.
- [19] G. Singh, S. Singh, C. Prakash, R. Kumar, R. Kumar, and S. Ramakrishna, "Characterization of three dimensional printed thermal stimulus polylactic acid hydroxyapatite based shape memory scaffolds," Polymer Composites, vol. 41, no. 9, pp. 3871-3891, 2020.
- [20] C. Prakash et al., "Mechanical reliability and in vitro bioactivity of 3D-printed porous polylactic acidhydroxyapatite scaffold," Journal of Materials Engineering and Performance, vol. 30, no. 7, pp. 4946-4956, 2021.
- [21] C. Esposito Corcione, F. Gervaso, F. Scalera, F. Montagna, A. Sannino, and A. Maffezzoli, "The feasibility of printing polylactic acid nanohydroxyapatite composites using a low cost fused deposition modeling 3D printer," *Journal of Applied Polymer Science*, vol. 134, no. 13, 2017.
- [22] P. Song *et al.*, "Novel 3D porous biocomposite scaffolds fabricated by fused deposition modeling and gas foaming combined technology," *Composites Part B: Engineering*, vol. 152, pp. 151-159, 2018.

- [23] A. Dawood, B. M. Marti, V. Sauret-Jackson, and A. Darwood, "3D printing in dentistry," *British dental journal*, vol. 219, no. 11, pp. 521-529, 2015.
- [24] J. M. Nasereddin, N. Wellner, M. Alhijjaj, P. Belton, and S. Qi, "Development of a simple mechanical screening method for predicting the feedability of a pharmaceutical FDM 3D printing filament," Pharmaceutical research, vol. 35, no. 8, pp. 1-13, 2018.
- [25] A. J. Sheoran and H. Kumar, "Fused Deposition modeling process parameters optimization and effect on mechanical properties and part quality: Review and reflection on present research," *Materials Today:* Proceedings, vol. 21, pp. 1659-1672, 2020.
- [26] S. Khan, K. Joshi, and S. Deshmukh, "A comprehensive review on effect of printing parameters on mechanical properties of FDM printed parts," *Materials Today:* Proceedings, 2021.
- [27] J. Chacón, M. A. Caminero, E. García-Plaza, and P. J. Núnez, "Additive manufacturing of PLA structures using fused deposition modelling: Effect of process parameters on mechanical properties and their optimal selection," *Materials & Design*, vol. 124, pp. 143-157, 2017.
- [28] M. Ouhsti, B. El Haddadi, and S. Belhouideg, "Effect of printing parameters on the mechanical properties of parts fabricated with open-source 3D printers in PLA by fused deposition modeling," *Mechanics and Mechanical Engineering*, vol. 22, no. 4, pp. 895-907, 2018
- [29] A. A. Ansari and M. Kamil, "Effect of print speed and extrusion temperature on properties of 3D printed PLA using fused deposition modeling process," *Materials Today: Proceedings*, vol. 45, pp. 5462-5468, 2021.
- [30] E. Carlier et al., "Investigation of the parameters used in fused deposition modeling of poly (lactic acid) to optimize 3D printing sessions," *International Journal of Pharmaceutics*, vol. 565, pp. 367-377, 2019.
- [31] A. Pandzic, D. Hodzic, and A. Milovanovic, "EFFECT OF INFILL TYPE AND DENSITY ON TENSILE PROPERTIES OF PLAMATERIAL FOR FDM PROCESS," *Annals of DAAAM & Proceedings*, vol. 30, 2019.
- [32] R. Karthikeyan, R. Ranganathan, V. Sreebalaji, and S. Munusamy, "Exploring the Impact of Surface Modifications on the Mechanical Characteristics of Acrylonitrile Butadiene Styrene Parts Manufactured Using Fused Deposition Modeling 3D Printing," *Journal of Materials Engineering and Performance*, pp. 1-8, 2025.
- [33] Z. Xu, R. Fostervold, and S. M. J. Razavi, "Thickness effect on the mechanical behavior of PLA specimens fabricated via Fused Deposition Modeling," *Procedia* Structural Integrity, vol. 33, pp. 571-577, 2021.
- [34] S. Alsa'di, M. Zgoul, W.H. AlAlaween, and S. M. Al-Qawabah, "Examining and Modelling the Effects of 3D Fused Deposition Parameters," *ES Materials & Manufacturing*, vol. 25, p. 1197, 2024.
- [35] M. C. Dudescu, L. Racz, and F. Popa, "Effect of infill pattern on fatigue characteristics of 3D printed polymers," *Materials Today: Proceedings*, vol. 78, pp. 263-269, 2023.
- [36] S. A. Deomore and S. J. Raykar, "Multi-criteria decision making paradigm for selection of best printing parameters of fused deposition modeling," *Materials Today: Proceedings*, vol. 44, pp. 2562-2565, 2021.

- [37] S. J. Raykar and D. D'Addona, "Selection of best printing parameters of fused deposition modeling using VIKOR," *Materials Today: Proceedings*, vol. 27, pp. 344-347, 2020.
- [38] R. V. Pazhamannil, P. Govindan, and P. Sooraj, "Prediction of the tensile strength of polylactic acid fused deposition models using artificial neural network technique," *Materials Today: Proceedings*, vol. 46, pp. 9187-9193, 2021.
- [39] R. Teharia, R. M. Singari, and H. Kumar, "Optimization of process variables for additive manufactured PLA based tensile specimen using taguchi design and artificial neural network (ANN) technique," *Materials Today: Proceedings*, 2021.
- [40] D. Yadav, D. Chhabra, R. K. Garg, A. Ahlawat, and A. Phogat, "Optimization of FDM 3D printing process parameters for multi-material using artificial neural network," *Materials Today: Proceedings*, vol. 21, pp. 1583-1591, 2020.
- [41] J. Giri, P. Shahane, S. Jachak, R. Chadge, and P. Giri, "Optimization of FDM process parameters for dual extruder 3d printer using Artificial Neural network," *Materials Today: Proceedings*, vol. 43, pp. 3242-3249, 2021.
- [42] W.H. AlAlaween, A. Alalawin, B. M. Y. Gharaibeh, M. Mahfouf and A. Alsoussi, "An Interval Type-2 Fuzzy Logic System for the Simulation of Fused Deposition," 2022 International Conference on Electrical, Computer, Communications and Mechatronics Engineering (ICECCME), Maldives, Maldives, 2022, pp. 1-6.
- [43] W.H. AlAlaween *et al.*, "The development of a radial based integrated network for the modelling of 3D fused deposition," *Rapid Prototyping Journal*, vol. ahead-of-print, no. ahead-of-print, 2022, doi: 10.1108/RPJ-04-2022-0121.
- [44] M. Lalegani Dezaki, M. K. A. Mohd Ariffin, and S. Hatami, "An overview of fused deposition modelling (FDM): Research, development and process optimisation," *Rapid Prototyping Journal*, vol. 27, no. 3, pp. 562-582, 2021.
- [45] W. H. AlAlaween *et al.*, "Fuzzy particle swarm for the right-first-time of fused deposition," *Journal of Intelligent & Fuzzy Systems*, vol. 45, no. 6, pp. 11977-11991, 2023.
- [46] W. H. AlAlaween, A. H. AlAlawin, L. Al-Durgham, and N. T. Albashabsheh, "A new integrated modelling architecture based on the concept of the fuzzy logic for the turning process," *Journal of Intelligent & Fuzzy* Systems, no. Preprint, pp. 1-13, 2021.
- [47] W. H. Alalaween, A. H. Alalawin, M. Mahfouf, and O. H. Abdallah, "A Dynamic Type-1 Fuzzy Logic System for the Development of a New Warehouse Assessment Scheme," *IEEE Access*, vol. 9, pp. 43611-43619, 2021.
- [48] W. H. AlAlaween *et al.*, "A dynamic nonlinear autoregressive exogenous model for the prediction of COVID-19 cases in Jordan," *Cogent Engineering*, vol. 9, no. 1, p. 2047317, 2022.
- [49] A. H. AlAlawin, W.H. AlAlaween, M. A. Salem, M. Mahfouf, N. T. Albashabsheh, and C. He, "A fuzzy logic based assessment algorithm for developing a warehouse assessment scheme," *Computers & Industrial Engineering*, vol. 168, p. 108088, 2022.
- [50] M. Alshafiee *et al.*, "A predictive integrated framework based on the radial basis function for the modelling of

- the flow of pharmaceutical powders," *International journal of pharmaceutics*, vol. 568, p. 118542, 2019.
- [51] W. H. AlAlaween, B. Khorsheed, M. Mahfouf, G. K. Reynolds, and A. D. Salman, "An interpretable fuzzy logic based data-driven model for the twin screw granulation process," *Powder Technology*, vol. 364, pp. 135-144, 2020.
- [52] W. H. AlAlaween, M. Mahfouf, and A. D. Salman, "When swarm meets fuzzy logic: Batch optimisation for the production of pharmaceuticals," *Powder Technology*, vol. 379, pp. 174-183, 2021.
- [53] W. H. AlAlaween, M. Mahfouf, and A. D. Salman, "Integrating the physics with data analytics for the hybrid modeling of the granulation process," AIChE Journal, vol. 63, no. 11, pp. 4761-4773, 2017.
- [54] A. Frikha and H. Moalla, "Analytic hierarchy process for multi-sensor data fusion based on belief function theory," *European Journal of Operational Research*, vol. 241, no. 1, pp. 133-147, 2015.
- [55] C. M. Bishop and N. M. Nasrabadi, *Pattern recognition and machine learning* (no. 4). Springer, 2006.
- [56] A. O. Boudraa, L. Bentabet, and F. Salzenstein, "Dempster-Shafer's basic probability assignment based on fuzzy membership functions," *ELCVIA: electronic letters on computer vision and image analysis*, pp. 1-10, 2004.
- [57] A. Maseleno, M. M. Hasan, N. Tuah, and C. R. Tabbu, "Fuzzy logic and mathematical theory of evidence to detect the risk of disease spreading of highly pathogenic avian influenza H5N1," *Procedia Computer Science*, vol. 57, pp. 348-357, 2015.
- [58] J. M. Mendel, Uncertain rule-based fuzzy logic systems: Introduction and new directions. Prentice Hall,
- [59] Q. Zhang and M. Mahfouf, "A hierarchical Mamdanitype fuzzy modelling approach with new training data selection and multi-objective optimisation mechanisms: A special application for the prediction of mechanical properties of alloy steels," *Applied soft computing*, vol. 11, no. 2, pp. 2419-2443, 2011.